Journal of Inflammation Research

Dovepress
Taylor & Francis Group

Open Access Full Text Article

ORIGINAL RESEARCH

Wheat-Grain Moxibustion Ameliorates Ulcerative Colitis: Suppressing Intestinal Inflammation, Modulating Gut Microbiota, and Restoring Mucosal Barrier Integrity

Tao Zhu[1,*], Shi-yue Sun[2,*], Shuo-xin Yang[3], Yu-fang Ji[3], Hong-ye Wan[2], Lai-xi Ji[3]

[1]School of Acu-Mox and Tuina, Chengdu University of Traditional Chinese Medicine, Chengdu, People's Republic of China; [2]Institute of Acupuncture and Moxibustion, China Academy of Chinese Medical Sciences, Beijing, People's Republic of China; [3]School of Acu-Mox and Tuina, Shanxi University of Chinese Medicine, Jinzhong, People's Republic of China

*These authors contributed equally to this work

Correspondence: Lai-xi Ji, School of Acu-Mox and Tuina, Shanxi University of Chinese Medicine, Jinzhong, 030600, People's Republic of China, Email jilaixi1964@163.com; Hong-ye Wan, Institute of Acupuncture and Moxibustion, China Academy of Chinese Medical Sciences, Beijing, 100700, People's Republic of China, Email redleaf2011@163.com

Background: Wheat-grain moxibustion (Wgm), a specialized form of moxibustion therapy, exerts therapeutic effects by delivering thermal stimulation from ignited moxa wool to specific acupoints, thereby preventing or treating various diseases. Previous studies have demonstrated its beneficial role in ulcerative colitis (UC); however, the exact mechanisms involved remain to be elucidated. This study investigated the therapeutic effects of Wgm at Zhongwan (CV12), Tianshu (ST25), and Shangjuxu (ST37) sites on colonic inflammatory cytokines, intestinal mucosal barrier homeostasis, and gut microbiome profiles in UC mice.

Materials and Methods: A DSS-induced UC mouse model was established and Wgm at Zhongwan (CV12), Tianshu (ST25), and Shangjuxu (ST37) acupoints was conducted once a day for 7 consecutive days. The therapeutic effects of Wgm were assessed by monitoring body weight variations, disease activity index (DAI) scoring, colon length measurements, and histopathological features of colonic tissues, and the expression levels of inflammatory cytokines and intestinal mucosal barrier-related factors in colonic tissues were measured using enzyme-linked immunosorbent assay (ELISA), immunohistochemistry (IHC), Western blotting (WB), and real-time quantitative polymerase chain reaction (RT-PCR). Additionally, 16S rRNA sequencing was performed to characterize the gut microbial community structure and diversity.

Results: Wgm applied to Zhongwan (CV12), Tianshu (ST25), and Shangjuxu (ST37) significantly reduced the DAI and histological scores of colonic tissue in UC mice, while demonstrating specific efficacy in increasing body weight and colon length. By inhibiting the TLR4/MyD88/NF-κB signaling pathway, Wgm suppressed the release of intestinal inflammatory cytokines (IL-1β, IL-6, IL-8, TNF-α, MPO, and COX2), downregulated intestinal injury markers (DAO, D-LA, ICAM-1, and IFABP), and upregulated mucosal barrier proteins (MUC2, ZO-1, Occludin, Claudin 1), thereby restoring intestinal mucosal barrier function and restoring the composition and diversity of the gut microbiota.

Conclusion: Our results suggest that Wgm alleviates colitis by suppressing the TLR4/MyD88/NF-κB signaling pathway, reducing pro-inflammatory cytokine release, restoring intestinal mucosal barrier integrity, and modulating gut microbiome profiles. These findings collectively elucidate the potential therapeutic mechanisms by which Wgm ameliorates UC pathogenesis and demonstrate its multimodal regulatory effects in UC.

Keywords: ulcerative colitis, wheat-grain moxibustion, intestinal flora, TLR4/MyD88/NF-κB signaling pathway, intestinal mucosal barrier

Introduction

Ulcerative Colitis (UC), a chronic non-specific inflammatory bowel disease with an increasing and younger incidence rate, usually occurs in the mucosa and submucosa of the colon and rectum with clinical manifestations such as weight

Received: 15 May 2025
Accepted: 5 September 2025
Published: 12 September 2025

loss, bloody stool, abdominal pain, diarrhea, etc.[1,2] Although commonly used clinical treatments, including mesalazine, 5-aminosalicylic acid, steroids, immunomodulators, and newly-developed nanoagents, can alleviate inflammatory responses in the short term, long-term use is prone to cause various adverse reactions.[3,4] Currently, there are no specific therapy for UC.[5,6] Therefore, more effective and safer treatment methods are necessary to reduce side effects and improve long-term efficacy.

The pathogenesis and progression of UC involves multifactorial interactions, including epithelial barrier dysfunction, immune dysregulation, environmental triggers, and gut microbiota alterations.[7–9] Among these, the excessive activation of inflammatory responses has been identified as a pivotal driver of UC pathogenesis.[10] The TLR4/MyD88/NF-κB, a canonical pro-inflammatory cascade, serves as a central regulator of intestinal inflammation by transcriptionally activating downstream effectors, such as cytokines (eg, TNF-α and IL-6), chemokines (CXCL8), and adhesion molecules (ICAM-1).[11] TLR4, the first identified Toll-like receptor (TLR) protein, mediates innate immune activation.[12] When TLR4 binds to its ligand, it initiates a downstream signaling cascade involving MyD88-dependent NF-κB nuclear translocation. This process promotes the secretion of primary inflammatory cytokines (IL-1β and TNF-α), which in turn stimulate secondary cytokine production (IL-6 and IL-8), thereby amplifying the inflammatory milieu.[13] Dysregulated release of these cytokines compromises intestinal barrier integrity, facilitating the translocation of luminal pathogens, toxins, and noxious substances into the submucosal layer, thereby perpetuating mucosal inflammation and establishing a self-perpetuating cycle of "inflammation-barrier disruption".[14,15] Consequently, mitigating intestinal inflammation and repairing compromised mucosal barriers are critical therapeutic strategies for UC. However, the mechanisms by which wheat-grain moxibustion (Wgm) modulates the inflammatory responses and protects the intestinal barrier in UC remain unclear.

Gut microbiota has emerged as a pivotal research focus in recent years, orchestrating bidirectional host-microbe crosstalk through multifaceted signaling networks, including metabolite-sensing receptors, pattern recognition receptors, and neuroendocrine pathways, which collectively maintain intestinal homeostasis by balancing immune activation, epithelial regeneration, and microbial colonization resistance.[16,17] The gut harbors approximately 10,000 resident microbial communities, whose composition and structure are dynamically regulated by various environmental factors.[9,18] The imbalance of intestinal microecology, characterized by a reduction in microbial diversity and disruption of microbial community stability, are significant pathological indications for the onset of colitis.[19] Studies have demonstrated that UC patients exhibit significantly diminished gut microbiota alpha diversity compared to healthy people, marked by a reduced abundance of probiotics (eg, Bifidobacterium and Lactobacillus) and overgrowth of potentially pathogenic bacteria (eg, Escherichia coli and Clostridium).[20,21] Compromised barrier integrity exacerbates the intestinal internal environment, further disrupting microbial balance, while dysbiotic microbiota perpetuate inflammation via immune activation and metabolic disturbances. This mutually reinforcing cycle of "inflammatory amplification-barrier disruption-dysbiosis" plays a central role in UC pathogenesis.[22,23] Consequently, multi-target intervention strategies for this system (including microbiota regulation, inflammation suppression, and barrier repair) have become key research priorities in UC treatment. Moxibustion therapy ameliorates colitis-associated pathologies in murine models by remodeling the gut microbial communities. Whether Wgm, a specialized traditional therapy, exerts its benefits through multi-dimensional regulation of this pathological network remains to be elucidated.

As a cornerstone of traditional Chinese medicine (TCM) with a millennia of clinical heritage, moxibustion exerts its therapeutic effects through the application of controlled thermal stimulation to specific acupoints, thereby harmonizing the flow of qi (vital energy) and blood.[24] Recent advancements in integrative medicine have propelled moxibustion into the spotlight of biomedical research owing to its noninvasive nature, minimal adverse effects, and empirically validated efficacy across inflammatory and immune-mediated conditions. Among its diverse modalities, Wgm represents a refined technique characterized by the strategic placement of ignited moxa wool pellets (2–3 mm in diameter) on acupoints, delivering localized heat penetration to achieve therapeutic objectives.[25] This modality synergizes the biomechanical effects of thermal energy with neuroimmunomodulatory responses, offering a unique interface between ancient practices and the modern pathophysiology. Accumulating evidence from both clinical trials and preclinical studies indicate that Wgm has broad anti-inflammatory effects on UC.[26,27] Our previous study demonstrated that Wgm applied to the acupoints Zhongwan (CV12), Tianshu (ST25), and Shangjuxu (ST37) effectively attenuated dextran sulfate sodium (DSS)-induced ulcerative colitis in

mice by suppressing the JAK2/STAT3 pathway, a key axis driving Th17-mediated inflammation.[28] However, the ecological interplay between Wgm and gut microbiota remains unexplored. Building on our previous findings and guided by the theory of acupoint selection in traditional Chinese medicine, this study employed Zhongwan (CV12), Tianshu (ST25), and Shangjuxu (ST37) as the primary therapeutic acupoints for UC. We aimed to elucidate the mechanisms involved in mitigating inflammation, restoring intestinal mucosal barrier integrity, and regulating gut microbiota composition, thereby advancing our understanding of their biological foundations and clinical relevance in colitis management.

Materials and Methods

Experimental Animals and Groups

In this study, 30 healthy SPF-grade C57BL/6J male mice with a body weight of 16–18g and an age of 6–8 weeks were housed in the Acupuncture and Moxibustion Laboratory of Shanxi University of Chinese Medicine. All the mice had free access to food (conventional experimental animal feed) and drinking water. The facility maintained a 12-hour light/dark cycle, controlled ambient temperature (22–25°C), and humidity (45–55%). The experiments commenced after a 7-day acclimatization period. All animal experiments were strictly in accordance with the regulations and provisions of the Animal Ethics Committee of Shanxi University of Chinese Medicine to ensure that all operations met ethical standards. (Ethical Approval No. 2019DW233).

The UC mouse model was induced by freely drinking 3% DSS (MP Biomedicals, California, USA) solution for 7 days,[29] and 20 mice were divided into two groups, namely the model group (Mod group, n=10) and the Wgm group (n=10), according to the random number table method. Mice in the control group (Con group, n=10) freely drank sterile distilled water. Diarrhea, weight loss, loose feces, and positive fecal occult blood in mice were the criteria for successful modeling[30] (Figure 1A).

Wgm Intervention

For the mice in the Wgm group, treatment was performed in accordance with the acupoint protocol outlined in "Experimental Acupuncture Science" by Professor Li Zhongren.[31] The detailed operational procedures are as follows. First, the hair was shaved at the acupoints Zhongwan (CV12), bilateral Tianshu (ST25), and bilateral Shangjuxu (ST37) to facilitate precise moxa application. Moxa velvet (Nanyang Kangaiduo Wormwood Products Co., Ltd, Nanyang, Henan, China) was then made into a moxa cone with a grain size of wheat (about 5 mg/grain). A thin layer of Vaseline was applied to each acupoint to prevent skin burns, and the moxa cone was then placed on the prepared area and ignited with an incense stick. The remaining moxa wool was immediately removed when a strong body twisting response was observed. Each acupoint received three consecutive stimulations (approximately 30s per session), repeated daily for seven days (Figure 1B). In the Con and Mod groups, the mice underwent identical handling and restraint procedures without moxibustion intervention to minimize stress-related confounding variables.

Body Weight and General Conditions Monitoring

From the initiation of modeling, body weight changes and survival status of mice in each group were measured and assessed every other day at 8:00 a.m.

Disease Activity Index (DAI)

On the 15th day of the experiment, the body weight, fecal characteristics, and degree of hematochezia were observed, and the Disease Activity Index (DAI) was scored.[32] DAI score = (weight loss score + stool consistency score + bloody stool score) /3. Body weight loss fraction (%) = (body weight after the last intervention–initial body weight)/initial body weight ×100. Detailed information on DAI is provided in Supplementary Table 1.

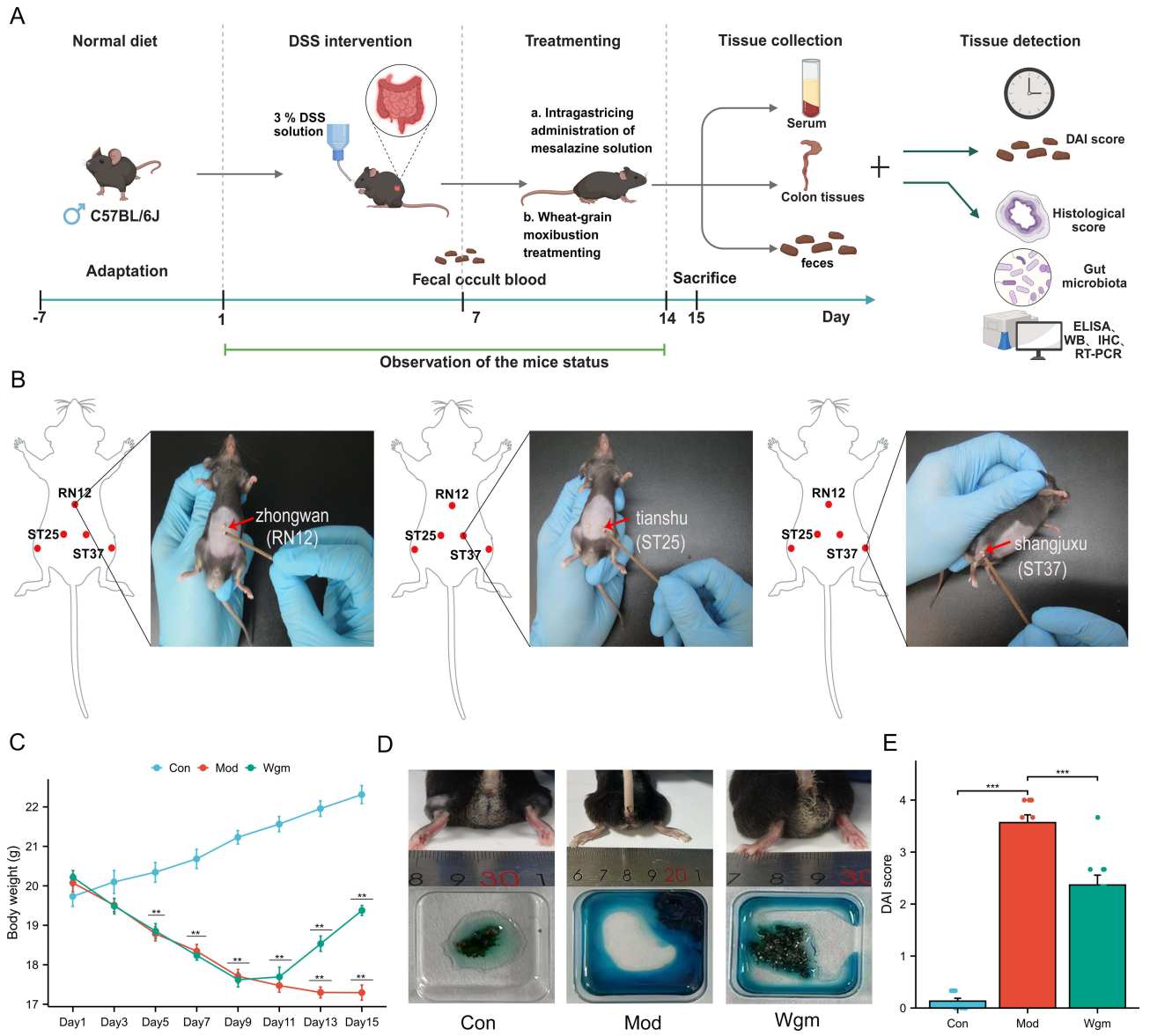

Figure 1 The UC mice model was established using 3% DSS solution. Wgm intervention was applied to Zhongwan (CV12) and bilateral Tianshu (ST25) and Shangjuxu (ST37) acupoints, administered once daily for 7 consecutive days. Body weight changes and general survival conditions of mice in each group were monitored and recorded daily throughout the experimental period. On day 15, a systematic assessment was performed, evaluating body weight, stool consistency, and fecal bleeding severity and quantitative scores were given based on the Disease Activity Index (DAI) criteria. Comprehensive analysis of the therapeutic effects of Wgm on colonic lesions in UC model mice was conducted through multidimensional assays. (**A**) Experimental design process. (**B**) Experimental operation of Wgm treatment. (**C**) Change in body mass (n=10). (**D**) Appearance of the mouse anus and fecal occult blood test. (**E**) DAI score (n=10). Data are expressed as mean ± SEM. n=10. ***P*<0.01, ****P*<0.001.

Colon Length, Intestinal Weight Index and Colon Mucosa Damage Index (CMDI) Score

Following the intervention period, the mice were euthanized and the colonic tissues were dissected for macroscopic evaluation. Colon length was measured, and the Intestinal Weight Index was calculated as follows: intestinal weight index (%) = [Colon Weight (g) ÷ Mouse Body Weight (g)] × 100%.

Collected colonic tissues were incised along the longitudinal axis of mesenteric arteries. The tissue samples were rinsed with ice-cold physiological saline to remove luminal contents. Gross pathological features including ulceration, erythema, and mucosal edema were visually assessed. Mucosal damage severity was scored according to the validated Colonic Mucosal Damage Index (CMDI) criteria.[33] The scoring criteria are provided in Supplementary Table 2.

Histopathological Examination of Colonic Tissues

The colonic tissues of the mice were fixed in 4% paraformaldehyde for 24 h, followed by standardized paraffin embedding through graded ethanol dehydration, xylene clearing, and paraffin infiltration. Paraffin wax blocks into 5μm sections. Deparaffinization was performed using xylene and rehydration was achieved using a descending ethanol gradient. Tissue morphology was evaluated using hematoxylin and eosin (H&E) staining. Following gradient dehydration in 95% ethanol and clearing in xylene, sections were mounted with neutral balsam. Histopathological changes were observed using optical microscopy. Colonic lesions were scored according to the Geboes scoring system and the average score result was taken.[34] The scoring criteria are provided in Supplementary Table 3.

Enzyme-Linked Immunosorbent Assay (ELISA)

Colonic tissues and serum samples were collected from mice. Following the manufacturer's protocols of ELISA kits, serum levels of ICAM-1 (KE10129, Proteintech), IFABP (E-EL-M0735, Elabscience), DAO (E-EL-M0412, Elabscience), and D-LA (E-BC-K002-M, Elabscience) were measured. Inflammatory cytokines in colonic tissues, including IL-1β (KE10003, Proteintech), TNF-α (E-EL-M3063, Elabscience), IL-6 (E-EL-M0044, Elabscience), and IL-8 (KGC1213-96, KGI Bio), were quantified. Optical density (OD) measurements at 450 nm were performed using a microplate reader (800TS, Biotek Instruments, Inc)., and the concentrations of serum and colonic biomarkers were calculated based on standard curves.

Immunohistochemical (IHC)

Colon tissues were fixed in 4% paraformaldehyde, embedded in paraffin wax blocks, and sectioned at 5 μm thickness. Deparaffinization was performed using xylene, followed by progressive rehydration using ethanol gradient in distilled water. Antigen repair was performed in citrate buffer (pH 6.0) using microwave heating at 98°C. Tissue sections were subjected to endogenous peroxidase quenching by incubation in a 3% hydrogen peroxide (H_2O_2)/methanol solution for 10 min at 25°C, followed by non-specific protein blocking with 3% bovine serum albumin (BSA) for 50 min to minimize background interference. Primary antibodies (anti-MPO, anti-COX2, anti-MUC2, anti-ZO-1, anti-occludin, and anti-claudin 1) were diluted to optimal concentrations and incubated overnight at 4°C. The next day, sections were incubated with secondary antibodies at room temperature for 50 min. Chromogenic development was initiated with DAB substrate under microscopic monitoring. Nuclear counterstaining was performed using hematoxylin, followed by differentiation in 1% acid ethanol and bluing in 0.2% ammonia water. The sections were sequentially dehydrated using a graded ethanol series, cleared in xylene, and permanently mounted with neutral balsam under coverslips. Histopathological evaluation was performed using a motorized optical microscope (BX51; Olympus, Tokyo, Japan). Positive cells were quantified by randomly selecting three fields of view and the mean optical density was calculated using ImagePro Plus 6.0. The detailed antibody concentrations are provided in Supplementary Table 4.

Western Blot (WB)

An appropriate amount of mouse colon tissue was collected and 100 μL lysis buffer, 1 μL broad-spectrum enzyme inhibitor, and 1 μL phosphatase inhibitor were added in proportion. The tissues were mechanically disrupted, the supernatant was collected at 12,000 rpm for 15 min, and the protein concentration was quantified with BCA assay. Proteins were separated by sodium dodecyl sulfate-polyacrylamide gel electrophoresis (SDS-PAGE) and transferred to 0.45 μm nitrocellulose membranes. The membranes were blocked with 5% skim milk for 1 h and incubated overnight at 4°C with primary antibodies (anti-ZO-1, anti-Occludin, anti-Claudin 1, anti-TLR4, anti-MyD88, anti-NF-κB p65, NF-κB p65, anti-β-actin). Following primary antibody incubation, the membranes were incubated with horseradish peroxidase (HRP)-conjugated species-matched secondary antibodies for 2 h at 25°C with gentle orbital shaking (50 rpm). Images were scanned and saved using a chemiluminescence/fluorescence image analysis system (5200Multi, Tanon, China). The relative expression levels of target proteins were semi-quantitatively analyzed using ImageJ software. Detailed antibody concentration information is provided in Supplementary Table 5.

Real-Time Quantitative Polymerase Chain Reaction (RT-qPCR)

Total RNA was extracted from colonic tissues using the TRIzol reagent kit, and its concentration and purity were determined using ultraviolet spectrophotometry. Total RNA was reverse transcribed into complementary DNA (cDNA) using a reverse transcription kit. Quantitative real-time PCR (qPCR) was performed in 20 μL reaction volumes containing 1 μL qPCR primers, 1 μL cDNA template, 10 μL SYBR Green qPCR Master Mix (2×), and 8 μL nuclease-free water. Amplification was conducted using the following thermal profile: initial denaturation at 95°C for 30s, 40 cycles of denaturation (95°C, 15s), combined annealing/extension (60°C, 30s), and melt curve analysis (60–95°C, 0.3°C/s increments). GAPDH served as the internal reference gene, and the relative mRNA expression levels of TLR4, MyD88, and NF-κB p65 were calculated using the $2^{-\Delta\Delta Ct}$ method. The detailed primer sequences are shown in Supplementary Table 6.

16S rRNA Sequencing

Fecal samples from each group were collected and total genomic DNA was extracted using a modified CTAB/SDS protocol with bead-beating homogenization. DNA concentration and purity were verified by 1.2% agarose gel electrophoresis with a λ-HindIII digest as a molecular weight marker. The hypervariable V3-V4 regions of the bacterial 16S rRNA genes were amplified using barcoded universal primers: the forward primer was 338F (5'-ACTCCTACGGGAGGCAGCA-3') and the reverse primer was 806R (5'-GGACTACHVGGGTWTCTAAT-3'). The product was purified using Vazyme VAHTSTM DNA Clean Beads and quantitatively analyzed using the Quant-iT PicoGreen dsDNA Assay Kit. Sequencing libraries were prepared using the Illumina TruSeq® Nano DNA LT Library Prep Kit and sequenced on the Illumina NovaSeq platform using the NovaSeq 6000 SP Reagent Kit. Bioinformatic analysis was conducted according to standardized protocols from Beijing Biomarker Technologies Co., Ltd. Raw sequencing data were processed using the BMKCloud platform. α-Diversity metrics were calculated to evaluate the within-sample microbial diversity across the experimental groups. Results were visualized as boxplots using the R script, with statistical significance assessed by Kruskal–Wallis tests, followed by Dunn's post-hoc analysis incorporating the Benjamini-Hochberg false discovery rate (FDR) correction for multiple comparisons. β-Diversity analysis was used to compare the similarities in species diversity among the samples in each group and to identify the differential microbiota between groups. Differential gene analysis was performed on the sequencing data using algorithms such as DESeq2 and a corrected P value (FDR) < 0.05, which was considered statistically significant.

Statistical Analysis

The analysis was conducted using the GraphPad Prism 8 software (GraphPad Software, Inc., San Diego, California, USA). Normally distributed measurement data are expressed as the mean ± SEM and analyzed by one-way analysis of variance (ANOVA). Statistical significance is defined as follows: $^{ns}P > 0.05$, $^{*}P < 0.05$, $^{**}P < 0.01$, $^{***}P < 0.001$.

Results

Wgm Improves the General Conditions of UC Mice

To evaluate the protective effects of Wgm in DSS-induced UC mice, we dynamically evaluated colitis indicators, such as weight change, consistency of loose stool, hematochezia, and DAI. After DSS administration, the body weight of the mice decreased significantly (22.31±0.69 vs 17.29±0.58, $P < 0.01$) (Figure 1C), the perianal area was unclean, and the fecal occult blood test showed a strong positive result (Figure 1D). DAI scores increased (0.13±0.16 vs 3.57±0.45, $P < 0.001$) (Figure 1E). Wgm treatment significantly increased the body weight of mice (17.29±0.58 vs 19.38± 0.38, $P < 0.01$), and reduced DAI (3.57±0.45 vs 2.37±0.57, $P < 0.001$). Simultaneously, the fecal occult blood test showed weakly positive results.

Wgm Alleviates the Intestinal Symptoms in UC Mice

Colon length, intestinal weight index, colonic mucosal damage index (CMDI) score, and hematoxylin-eosin (H&E) staining were assessed to further evaluate the protective effects of Wgm in UC mice. The results revealed that the Mod

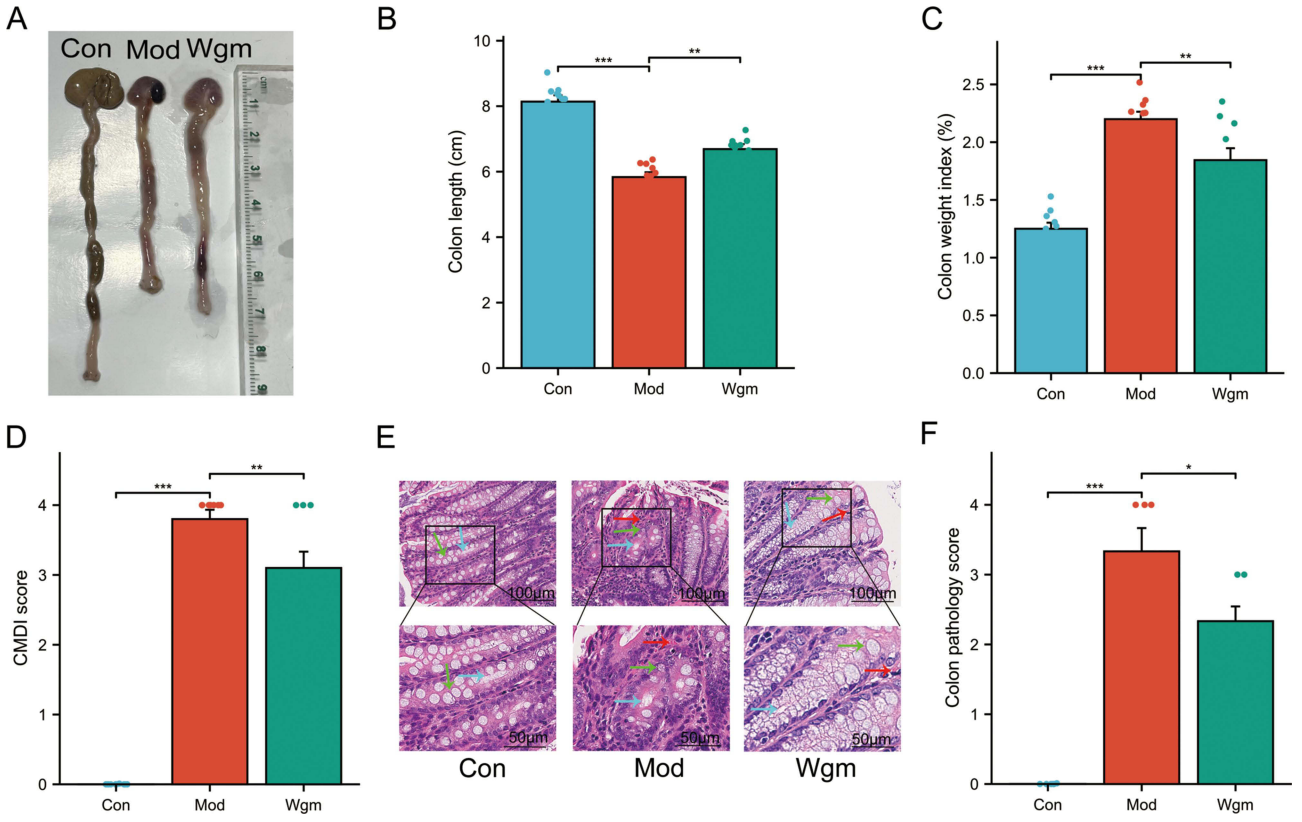

Figure 2 Wgm alleviates intestinal symptoms in UC mice. (**A**) Macroscopic view of colons. (**B**) Colon length (n=10). (**C**) Intestinal weight index (n=10). (**D**) Colonic mucosal damage index (CMDI) score (n=10). (**E**) Hematoxylin-eosin (H&E) staining of colonic tissues. Scale bars: 100 μm and 50 μm. Green arrows indicate glandular structures; blue arrows denote crypt structures; red arrows highlight inflammatory cell infiltration. (**F**) Histopathological scores of colonic tissues (n=6). Scale bar: 100 μm; 50 μm. Data are expressed as mean ± SEM. **P* < 0.05, ***P* < 0.01, ****P* < 0.001.

group exhibited a significantly shortened colon length (8.14±0.58 vs5.83±0.45, $P < 0.001$) (Figure 2A and B), increased intestinal weight index (1.25±0.16 vs 2.20±0.19, $P < 0.001$) (Figure 2C), elevated CMDI scores (0±0.00 vs 3.80±0.40, $P < 0.001$) (Figure 2D), and aggravated pathological damage (0±0.00 vs3.33±0.75, $P < 0.001$) (Figure 2E and F). In contrast, the Wgm group showed markedly ameliorated colon shortening (5.83±0.45 vs 6.69±0.46, $P < 0.001$), decreased intestinal weight index (2.20±0.19 vs 1.84±0.31, $P < 0.001$), reduced CMDI scores (3.80±0.40 vs 3.10±0.70, $P < 0.01$), improved intestinal mucosal morphology (3.33±0.75 vs 2.33±0.47, $P < 0.05$), and restored glandular and crypt structure. These findings suggest that Wgm effectively alleviated symptoms in mice with DSS-induced UC.

Wgm Alleviates Colonic Inflammation in UC Mice Through the TLR4/Myd88/NF-κB Signaling Pathway

Overexpression of inflammatory cytokines is a key driver of UC. Excessive immune responses triggered by pathogen infiltration into the lamina propria lead to the accumulation of pro-inflammatory factors (such as TNF-α, IL-1β, IL-6, IL-8, MPO, and COX2) in the gut, initiating a cascade of cellular events. The expression levels of these key molecules were measured to evaluate the effects of Wgm on colonic inflammation in DSS-induced UC mice.[35] The results demonstrated that Wgm reversed the DSS-induced upregulation of IL-1β, IL-6, IL-8, and TNF-α in the colon (Figure 3A–D). Immunohistochemical analysis revealed similar trends for MPO and COX2 expression (Figure 3E–H).

The TLR4/MyD88/NF-κB signaling pathway is closely associated with the secretion of pro-inflammatory cytokines (IL-1β, IL-6, IL-8, TNF-α, MPO, and COX2).[36] We hypothesized that Wgm ameliorates UC inflammation by modulating this pathway. To test this hypothesis, we examined TLR4 signaling activation and observed significantly elevated expression of TLR4, MyD88, and NF-κB p65 in DSS-induced colonic tissues (Figure 3I–O). However, Wgm treatment suppressed both the protein and mRNA levels of these signaling components. These data indicated that Wgm alleviates

https://doi.org/10.2147/JIR.S540574

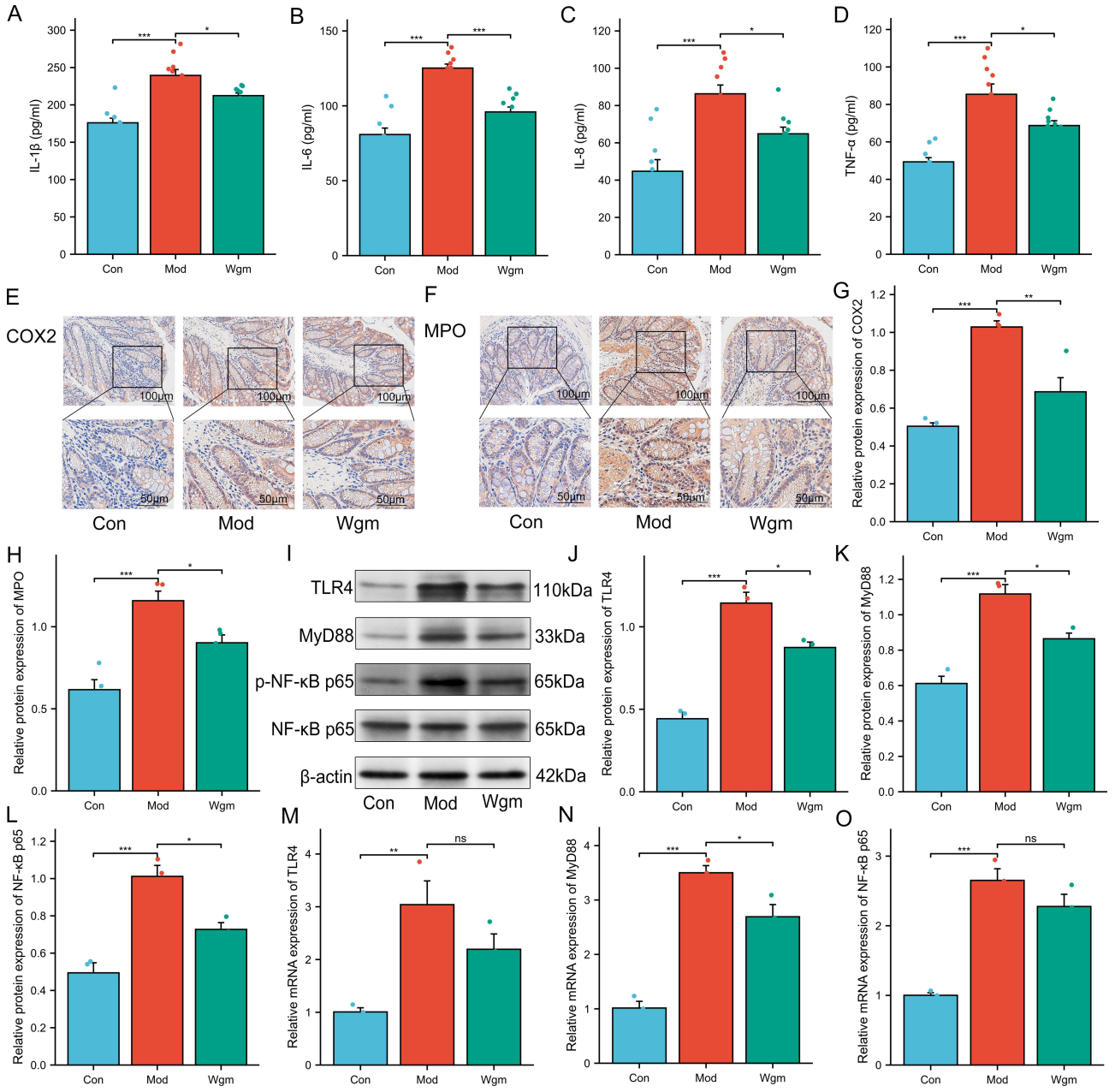

Figure 3 Wgm improves colonic inflammation in UC mice by suppressing the TLR4/MyD88/NF-κB signaling pathway. (**A**–**D**) Levels of IL-1β, IL-6, IL-8, and TNF-α in the colon (n=10). (**E**–**H**) Expression of COX2 and MPO in colon tissue (n=4), Scale bar: 100 μm; 50 μm. (**I**–**O**) Protein and mRNA levels of TLR4, MyD88, and NF-κB p65 in colonic tissues (n=3). Data are expressed as mean ± SEM. n=10. ^{ns}P >0.05, *P<0.05, **P<0.01, ***P<0.001.

ulcerative colitis-associated intestinal inflammation by suppressing the TLR4/MyD88/NF-κB pathway. Collectively, our findings demonstrated the robust efficacy of Wgm in mitigating intestinal inflammation in UC.

Wgm Improves the Intestinal Mucosal Barrier Integrity of UC Mice

Accumulation of intestinal inflammatory cytokines typically disrupts the intestinal mucosal mechanical barrier, which is the primary defense of the gut barrier, and functions through intestinal epithelial cells and tight junction proteins.[37] The serum levels of gut injury markers (DAO, D-LA, ICAM-1, and IFABP) and expression levels of tight junction proteins (MUC2, ZO-1, Occludin, Claudin 1) were measured to evaluate the effects of Wgm on intestinal barrier integrity. Results demonstrated that DSS-induced UC mice exhibited significantly increased serum DAO, D-LA, ICAM-1, and IFABP levels

(Figure 4A–D). Concurrently, colonic tissues displayed marked reductions in tight junction protein (Occludin, Claudin-1, ZO-1) and mucin MUC2 expression (Figure 4E–L). Notably, Wgm treatment effectively reversed these pathological alterations; the serum levels of these injury markers were significantly decreased, and the expression of tight junction

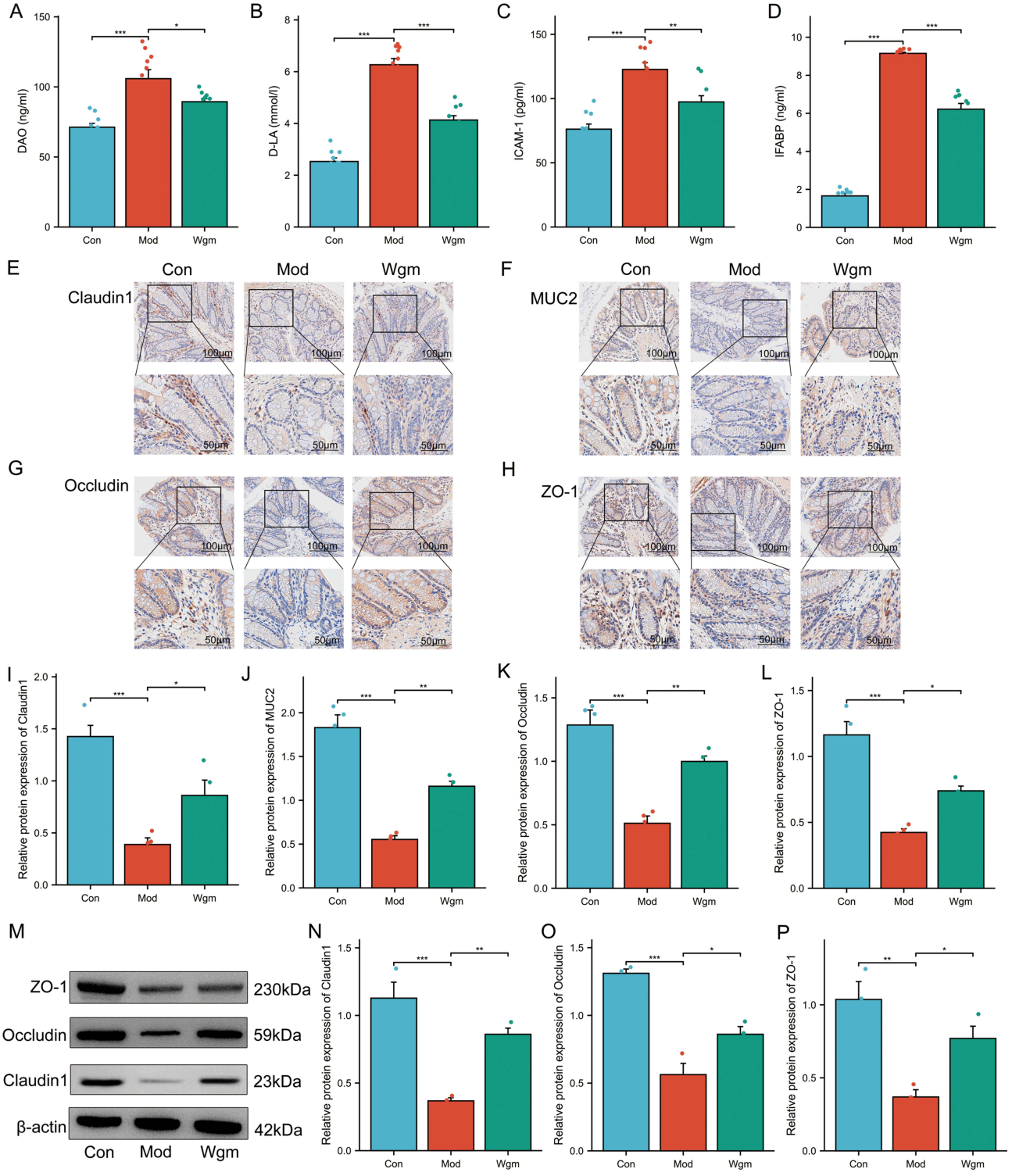

Figure 4 Wgm improves the intestinal mucosal barrier integrity in UC mice. (**A**–**D**) Serum levels of DAO, D-LA, ICAM-1, and IFABP (n=10). (**E**–**L**) Immunohistochemical analysis of Claudin 1, MUC2, Occludin, and ZO-1 in colonic tissues (n=4). Scale bars: 100 μm; 50 μm. (**M**–**P**) Western blot analysis of Claudin 1, Occludin, and ZO-1 expression in colonic tissues (n=3). Data are expressed as mean ± SEM. **P* < 0.05, ***P* < 0.01, ****P* < 0.001.

https://doi.org/10.2147/JIR.S540574

proteins was restored. WB analysis corroborated these findings (Figure 4M–P). Collectively, the enhanced expression of tight junction proteins in colonic tissues correlates with the protective effects of Wgm against DSS-induced UC.

Wgm Ameliorates Gut Microbiota Dysbiosis in UC Mice

Impaired intestinal barrier integrity and increased permeability allows gut bacteria to infiltrate the lamina propria, leading to microbial dysbiosis.[38] To investigate the association between the anti-inflammatory effects of Wgm and gut microbiota remodeling, we performed 16S rRNA gene sequencing of colonic contents, which revealed distinct operational taxonomic units (OTUs) across groups; 1066, 769, and 873 unique OTUs were identified in the Con, Mod, and Wgm groups, respectively (Figure 5A). The rank-abundance curves reflected species richness and evenness, which in each group were relatively wide and eventually tended to level off, indicating uniform and diverse microbial communities (Figure 5B and C). Alpha diversity indices were analyzed to evaluate the impact of Wgm's on microbial richness and diversity. The results showed reduced Chao 1, ACE, PD_whole_tree, Shannon, Coverage, and Simpson indices in the Mod group, whereas Wgm treatment significantly restored the structure and diversity of the gut microbial community. (Figure 5D–I). The Beta Diversity Index (PCA, PCoA, and NMDS) was used to reveal similarities and differences among the microbiota. These three indices revealed significant changes in the gut microbiota of DSS-induced mice, which were alleviated by Wgm (Figure 5J–L). These findings collectively demonstrate that Wgm restores gut microbiota composition in UC mice.

Wgm Increases the Species Abundance of the Gut Microbiota in UC Mice

To define the microbial composition, the top 10 most abundant gut microbiota in the phyla and genera were examined. Taxonomic profiling at the phylum level revealed that Wgm significantly increased the relative abundance of Firmicutes and reduced the abundance of Bacteroidetes and Proteobacteria in UC mice (Figure 6A–E). Taxonomic profiling at the genus level demonstrated that Wgm decreased the relative abundance of the Lachnospiraceae_NK4A136_group, but elevated the abundance of unclassified_Muribaculaceae and Akkermansia (Figure 6F–J). Collectively, these findings suggest that Wgm alleviates UC by modulating specific gut microbiota.

To further evaluate the impact of Wgm on the gut microbiota composition in UC mice, we performed LEfSe analysis and plotted the linear discriminant (LDA) (Figure 6K and L). Alloprevotella, Lachnospiraceae_FCS020_group, Blautia, and Enterococcus were the dominant taxa in DSS group. In contrast, Verrucomicrobiota and Akkermansia were the main bacteria in the Wgm group. Further analysis was performed using Picturst2 (Figure 6M), which predicted the metabolic pathways of the intersecting species using the KEGG database and revealed that the main metabolic pathways, biosynthesis of secondary metabolites, biosynthesis of antibiotics, and biosynthesis of amino acids were related. These results indicate that the biological functions of gut microbiota across groups are closely linked to metabolic pathways, suggesting that microbiota-host interactions in UC mice may be mediated by metabolic pathways.

The Correlation Between Gut Microbiota and Colonic Indicators

To investigate the potential correlations between gut microbiota and UC pathogenesis, Spearman correlation analysis was used to assess the relationships among gut microbial taxa, DAI scores, inflammatory cytokines, and tight junction proteins. The results demonstrated that Bacteroidetes and Lachnospiraceae_NK4A136_group exhibited significant negative correlations with body weight, colon length, and intestinal barrier proteins but positively correlated with pro-inflammatory cytokines and DAI scores (Figure 7A–C). These findings suggest that the preventive effects of Wgm against colitis in UC mice may involve the modulation of the gut microbiota.

Discussion

As a safe and traditional non-pharmacological therapy, Wgm has garnered extensive recognition owing to its dual anti-inflammatory and immunomodulatory properties in diverse immune-related disorders.[39] In this study, Wgm showed significant therapeutic efficacy in mice with DSS-induced UC (Figure 8). Histopathological analyses revealed that Wgm-treated mice exhibited preserved crypt architecture, reduced inflammatory cell infiltration, and attenuated epithelial erosion compared with the untreated model group, strengthening their capacity to counteract DSS-induced mucosal

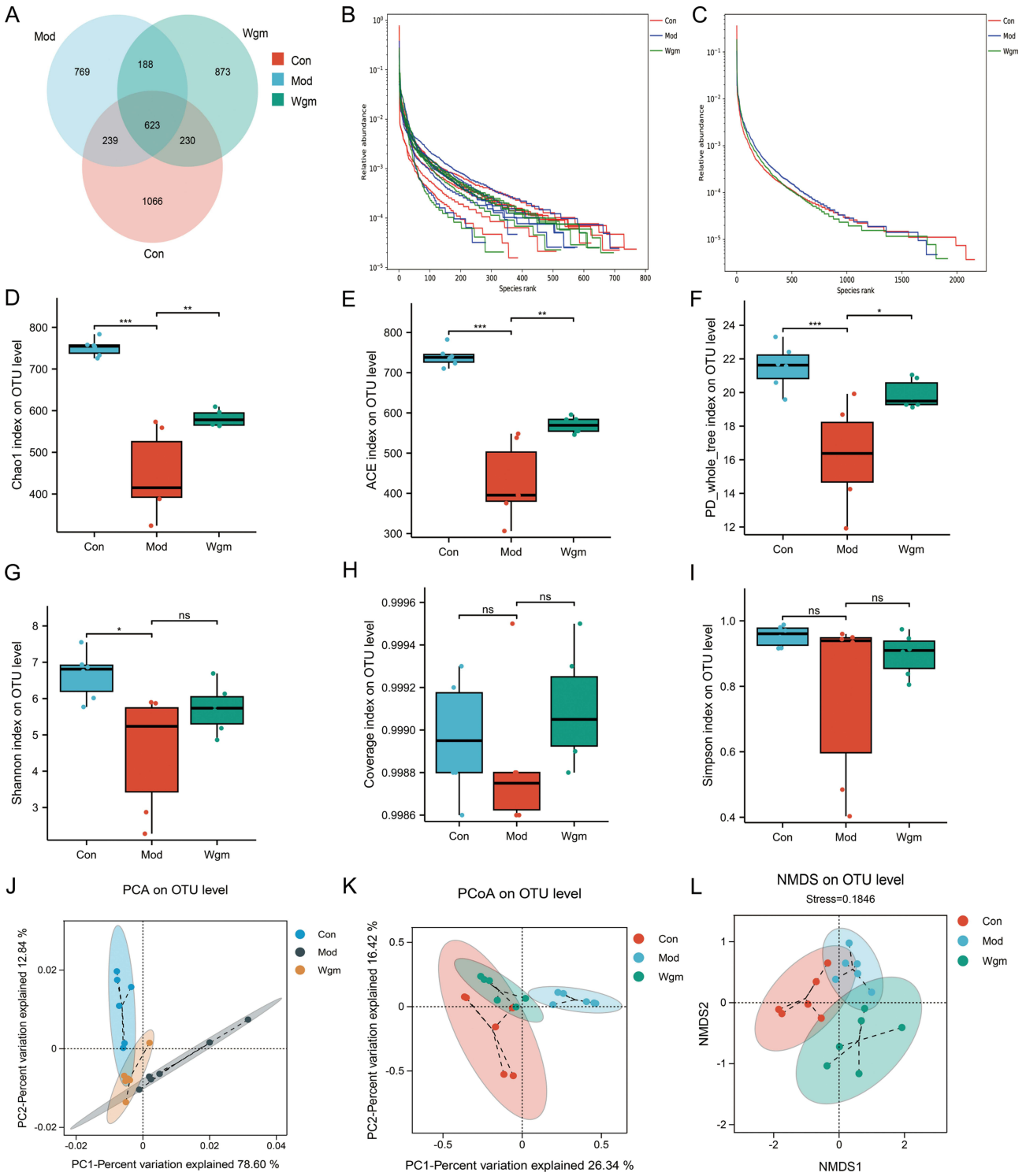

Figure 5 Wgm ameliorates gut microbiota dysbiosis in UC mice. (**A**) Venn diagram. (**B** and **C**) OTU Rank curve. (**D**) Chao 1 index (n=6). (**E**) ACE index (n=6). (**F**) PD_whole_tree index (n=6). (**G**) Shannon index (n=6). (**H**) Coverage index (n=6). (**I**) Simpson index (n=6). (**J**) PCA. (**K**) PCoA. (**L**) NMDS. Data are expressed as mean ± SEM. ^{ns}P >0.05, * P < 0.05, ** P < 0.01, *** P < 0.001.

injury. All findings demonstrated that Wgm treatment significantly ameliorated colitis severity, as evidenced by the restored colonic mucosal barrier integrity and mitigation of hallmark UC symptoms, including diarrhea, hematochezia, and pathological tissue damage. Further investigation indicated that UC progression was closely associated with hyperactivation of the TLR4/MyD88/NF-κB signaling pathway. Notably, Wgm markedly suppressed aberrant activation

https://doi.org/10.2147/JIR.S540574

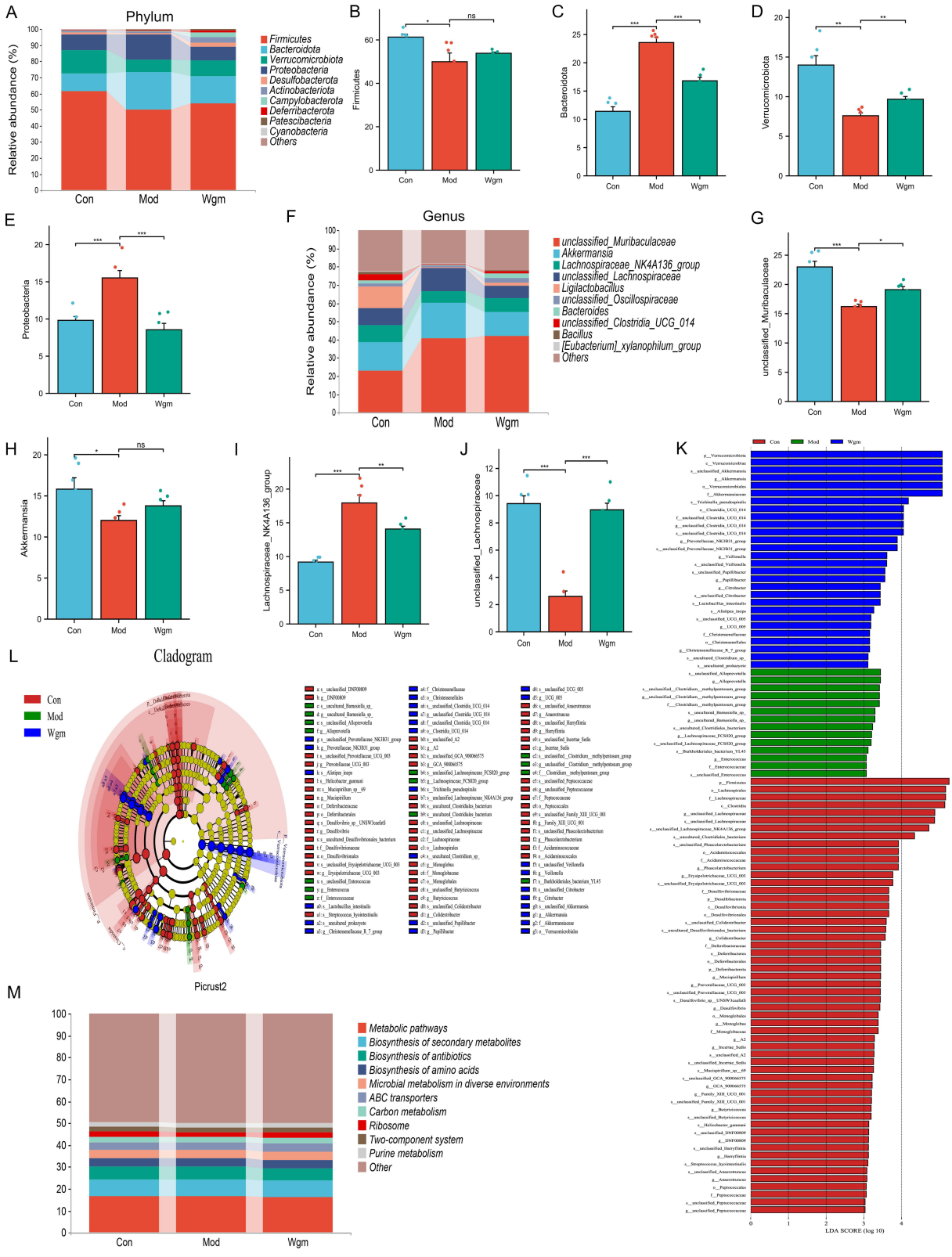

Figure 6 Wgm improves the species abundance of the gut microbiota in UC mice. (**A**) Phylum diagram. (**B**–**E**) Detection of Fimicutes, Bacteroidota, Verrucomicrobiota and Proteobacteria (n=6). (**F**) Genus diagram. (**G**–**J**) Detection of unclassified_Muribaculaceae, Akkermansia, Lachnosipiraceae_NK4A136_groupe (n=6). (**K**) LDA. (**L**) LefSe. (**M**) Picrust2. Data are expressed as mean ± SEM. ^{ns}P >0.05, * P < 0.05, ** P < 0.01, *** P < 0.001.

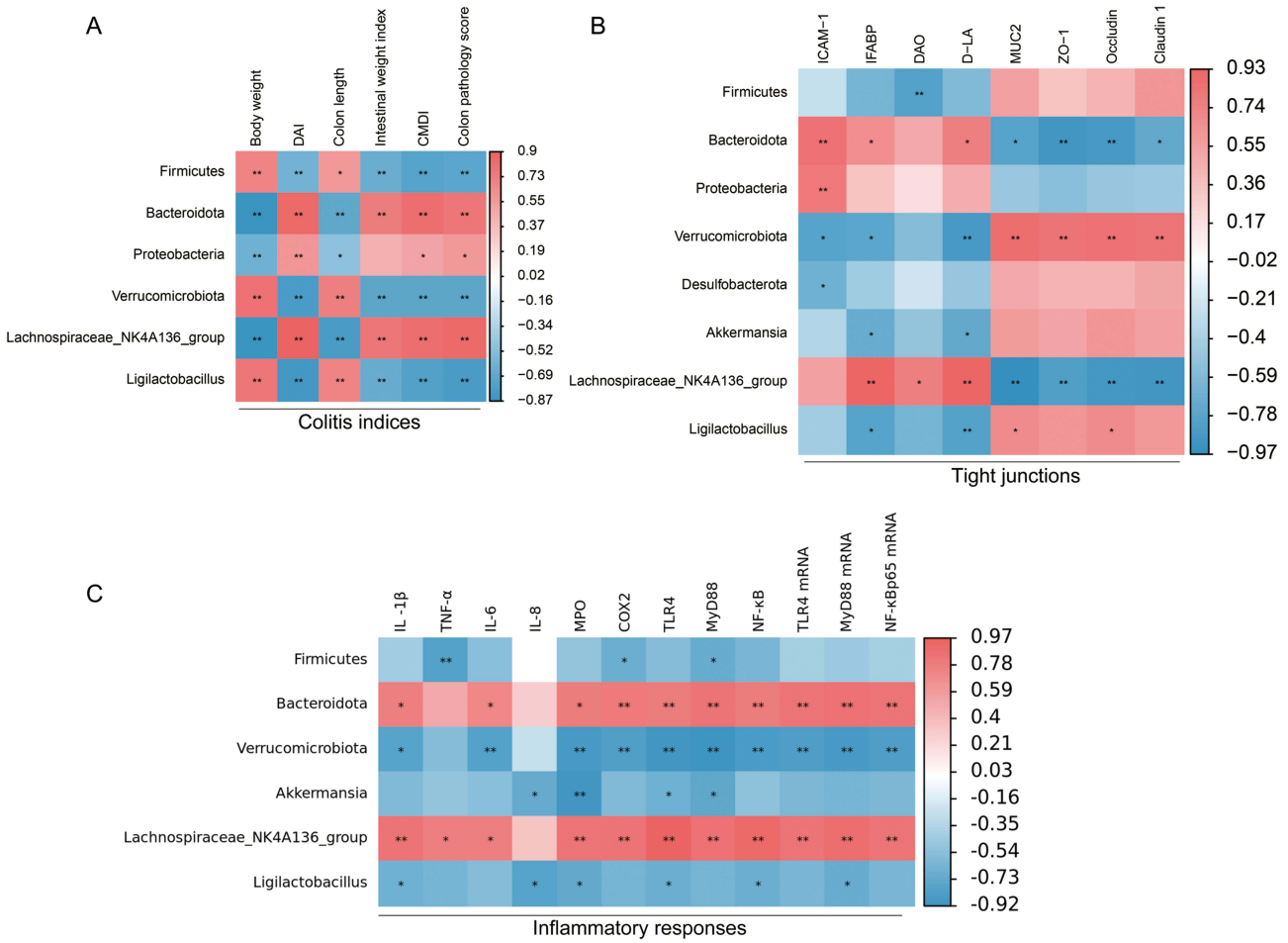

Figure 7 The correlation between gut microbiota and colonic indicators. (**A**) Spearman correlation analysis was used to analyze the relationship between intestinal flora and DAI score (n=6). (**B**) Spearman correlation analysis was used to analyze the relationship between intestinal flora and tight junction (n=3). (**C**) Spearman correlation analysis was used to analyze the relationship between intestinal flora and inflammatory markers (n=3). Positive and negative correlations are indicated in red and blue, respectively. **P*<0.05, ***P*<0.01.

of this pathway, significantly reducing pro-inflammatory cytokine levels, thereby attenuating excessive inflammatory responses. Additionally, Wgm reshaped the gut microbiota structure and increased the relative abundance of anti-inflammatory bacteria, synergistically enhancing the intestinal protection. To our knowledge, this study is the first to delineate the multi-target mechanisms of Wgm, simultaneously addressing inflammatory signaling, microbial dysbiosis, and mucosal repairing UC pathogenesis. These findings suggest that Wgm is a novel integrative therapeutic strategy that bridges traditional medical principles with modern molecular insights to improve UC management.

The DSS-induced UC mouse model is widely used in experimental research because of its high reproducibility, simplicity, and pathological resemblance to human UC.[40] In our study, characteristic DSS-induced pathological manifestations, including weight loss, colorectal shortening, mucosal edema, inflammatory cell infiltration, and crypt architectural destruction, were clearly observed. Interestingly, Wgm treatment significantly restored body weight, increased colon length, and reduced both DAI and histopathological scores in mice. Building on previous studies showing that TLR4/MyD88/NF-κB signaling is associated with intestinal inflammation in UC, we investigated the regulatory effects of Wgm on this pathway. TLR4 can upregulate the secretion of cytokines, including IL-1β, IL-6, IL-8, TNF-α, MPO, and COX2, by activating pathways, such as interleukin receptor-associated kinase and NF-κB, initiating intracellular signaling cascades that exacerbate colonic tissue damage. In general, Wgm-treated UC mice exhibited significantly lower colonic pro-inflammatory cytokine levels than the untreated model group, and mechanistic evidence points to TLR4/MyD88/NF-κB signaling pathway inhibition.

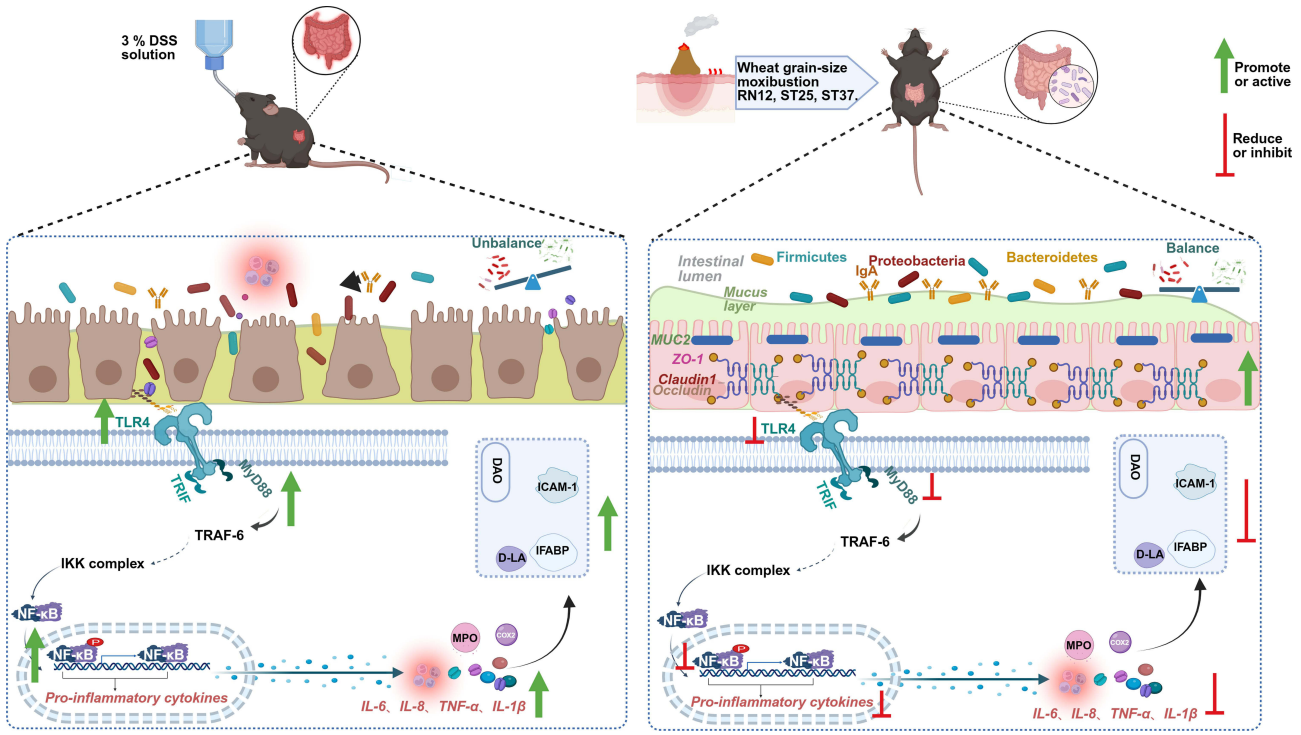

Figure 8 Wgm alleviates UC symptoms potentially by inhibiting the TLR4/MyD88/NF-κB signaling pathway to reduce the release of pro-inflammatory cytokines, repairing mucosal barrier damage, enhancing intestinal microbial diversity, and suppressing pathogenic bacterial proliferation.

Excessive expression and secretion of pro-inflammatory cytokines can trigger persistent inflammation, leading to colonic mucosal damage.[41,42] Under physiological conditions, the intestinal mucosal barrier selectively permits the passage of ions and small, soluble molecules.[43] Dysfunction of this barrier disrupts mucosal permeability and integrity, allowing harmful substances (macromolecules and microbes) or endotoxins to penetrate the intestinal wall and enter blood circulation. This process elevates serum levels of intestinal injury markers such as D-LA, DAO, and IFABP, thereby inducing inflammatory reactions.[44,45] Reducing pro-inflammatory factor expression to mitigate colonic inflammatory injury remains the primary strategy for alleviating UC symptoms.[46] D-LA, DAO, IFABP, and ICAM-1 are indirect indicators of impaired mucosal barrier function. The damaged barrier can lead to elevated D-LA, DAO, IFABP, and ICAM-1 levels; harmful bacteria in the intestine penetrate the intestinal wall and enter the bloodstream, impairing the mucus layer and the intestinal mucosal barrier.[47] Tight junction proteins, including ZO-1, Claudin 1, and occludin, are critical biomarkers for evaluating the mucosal barrier function. Reduced expression of these proteins reflects increased intestinal permeability, altered barrier integrity, and mucosal dysfunction.[48] In mice with DSS-induced UC, decreased MUC2 secretion and downregulated tight junction protein expression are observed, accompanied by heightened mucosal permeability.[49] Notably, Wgm treatment reversed these pathological alterations, demonstrating its efficacy in repairing colonic mucosal damage.

Furthermore, gut microbiota dysbiosis exacerbates intestinal barrier disruption, increases permeability, and amplifies inflammatory responses, ultimately driving the initiation and progression.[50] Thus, modulation of gut microbiota is a pivotal therapeutic target for UC prevention and management. In this study, the gut microbiota of mice was comprehensively evaluated. Compared with the Con group, the bacterial abundance in the Mod group was greatly reduced. However, Wgm treatment restored both Alpha and Beta diversities. PCA, PCoA, and NMDS analyses revealed obvious clustering between the model and control groups, which was attenuated by Wgm, indicating its potential to rebalance dysbiosis of the gut microbiota.

Phylum-level taxonomic analysis revealed that Wgm intervention induced significant microbial restructuring in UC mice, characterized by a substantial increase in Firmicutes abundance and an obvious elevation in Verrucomicrobiota.

Firmicutes, which are predominant in healthy human intestines, exert multimodal protective effects through dietary fiber fermentation, short-chain fatty acid (SCFA) biosynthesis, and immune modulation, which are critical for maintaining intestinal barrier integrity and suppressing inflammatory responses.[51] In patients with UC, reduced Firmicutes abundance correlates with diminished SCFA production, leading to compromised barrier function, increased permeability, and exacerbated inflammation.[52] Compared to the Con group, Wgm also markedly decreased the relative abundance of Bacteroidetes and Proteobacteria. Elevated levels of these bacteria are associated with UC severity. Bacteroidetes may promote UC progression by altering the gut microenvironment, disrupting the intestinal barrier function, and activating pro-inflammatory pathways.[53] Bacteroidetes may also affect the host immune response by generating metabolites that further exacerbate the intestinal inflammatory response.[54,55] Proteobacteria, a type of pathogenic bacteria linked to the regulation of intestinal epithelial dysfunction, is positively correlated with pro-inflammatory cytokine expression levels and key genes in the immune-inflammatory pathway. Their enrichment may exacerbate and maintain inflammation through endotoxin production, increased intestinal permeability, and host immune activation.[56] Thus, modulation of the Phylum-level microbiota composition by Wgm is closely associated with UC inflammatory resolution.

Genus-level taxonomic profiling revealed significant microbial dysbiosis in mice with DSS-induced colitis (Mod group), characterized by an obvious decline in the relative abundance of Akkermansia, unclassified_Muribaculaceae, and unclassified_ Lachnospiraceae and an increase in the relative abundance of Lachnospiraceae_NK4A136_group. Treatment with Wgm reversed these dysbiotic trends. Muribaculaceae, recognized as a probiotic, is crucial for maintaining gut health, reinforcing intestinal barrier function, and inhibiting pathogenic overgrowth.[57] This decrease may impair intestinal protective mechanisms and exacerbate microbial imbalance and inflammation.[58] Akkermansia, a common intestinal probiotic, increases intestinal barrier integrity and mitigates immune-inflammatory responses.[59] Studies have indicated that enrichment of Akkermansia is associated with SCFAs metabolism and is negatively correlated with pro-inflammatory cytokines, which could trigger significant anti-inflammatory effects and enhance intestinal epithelial barrier function, thereby alleviating intestinal inflammation and reducing intestinal injury.[60] Notably, the elevated LachnospiraceaeNK4A136group abundance may reflect inflammatory aggravation and altered SCFA production.[61] Therefore, gut microbiota significantly contributes to the occurrence and development of UC. Given the intricate interplay between gut microbiota and host immunity, inflammatory states may have an adverse effect on the balance of intestinal microbial equilibrium. These findings suggest that the beneficial reshaping of the gut microbiota composition by Wgm may synergize with its intrinsic anti-inflammatory properties to ameliorate UC.

This study is the first to demonstrate that Wgm alleviates UC in mice by suppressing hyperactivation of the TLR4/MyD88/NF-κB signaling pathway, thereby reducing pro-inflammatory cytokine release, mitigating inflammation, and restoring intestinal barrier function. Concurrently, Wgm intervention induced comprehensive restructuring of the gut microbial ecosystem, as evidenced by Phylum-level modulation and Genus-level reprogramming, particularly enriching beneficial microbiota abundance, reshaping microbial structure, and rebalancing intestinal immunity.

Collectively, these findings suggest that Wgm is a promising integrative therapy for UC, reducing its harm to the body. However, this study had several limitations. First, although we focused on the anti-inflammatory effects of Wgm via gut microbiota modulation, barrier restoration, and related inflammatory pathway inhibition, additional mechanisms against inflammation remain to be explored. Second, although TLR4/MyD88/NF-κB suppression partially explains the therapeutic efficacy of Wgm, the contribution of other pathways warrants further investigation. Finally, although Wgm demonstrates a clear therapeutic effect in the UC mouse model, a comprehensive safety assessment of its impact on various organs will be conducted in subsequent studies using a multifaceted analytical approach. This will provide more rigorous scientific evidence to support Wgm's clinical application. Future studies integrating molecular and systems biology approaches are needed to elucidate the multi-target, multi-pathway mechanisms of Wgm in UC management.

Conclusion

In conclusion, Wgm alleviated UC symptoms through four synergistic mechanisms: reducing the release of pro-inflammatory cytokines by inhibiting the TLR4/MyD88/NF-κB signaling pathway, repairing mucosal barrier damage, enhancing intestinal microbial diversity, and suppressing pathogenic bacterial proliferation. This study highlights Wgm as a safe and effective traditional Chinese medicine therapy, meriting its clinical translation for UC treatment.

Data Sharing Statement

The data supporting this study is available from Lai-xi Ji (E-mails: jilaixi1964@163.com) upon reasonable request.

Ethics Statement

Ethics approval and informed consent: All mouse protocols were approved by the Animal Welfare Committee of Shanxi University of Chinese Medicine (no. 2019DW233).

Author Contributions

All authors made a significant contribution to the work reported, whether that is in the conception, study design, execution, acquisition of data, analysis and interpretation, or in all these areas; took part in drafting, revising or critically reviewing the article; gave final approval of the version to be published; have agreed on the journal to which the article has been submitted; and agree to be accountable for all aspects of the work.

Funding

This study was supported by funds from the Natural Science Foundation of China (82205280, 82074549) and the Fundamental Research Funds for the Central Public Welfare Research Institutes (ZZ15-YQ-050).

Disclosure

The authors declare that they have no conflicts of interest to disclose.

References

1. Le Berre C, Honap S, Peyrin-Biroulet L. Ulcerative colitis. *Lancet*. 2023;402(10401):571–584. doi:10.1016/S0140-6736(23)00966-2
2. Voelker R. What Is Ulcerative Colitis? *JAMA*. 2024;331(8):716. doi:10.1001/jama.2023.23814
3. Li R, Fan Y, Liu L, et al. Ultrathin hafnium disulfide atomic crystals with ROS-scavenging and colon-targeting capabilities for inflammatory bowel disease treatment. *ACS Nano*. 2022;16(9):15026–15041. doi:10.1021/acsnano.2c06151
4. Liu L, Li R, Xie L, et al. Hafnium hydride Nanosheets with reactive oxygen and nitrogen species and cell-free DNA-dual scavenging capabilities for inflammatory bowel disease treatment. *J Colloid Interface Sci*. 2025;699(Pt 2):138222. doi:10.1016/j.jcis.2025.138222
5. Panés J, Alfaro I. New treatment strategies for ulcerative colitis. *Expert Rev Clin Immunol*. 2017;13(10):963–973. doi:10.1080/1744666X.2017.1343668
6. Calméjane L, Laharie D, Kirchgesner J, Uzzan M. Review article: updated management of acute severe ulcerative colitis: from steroids to novel medical strategies. *United Eur Gastroenterol J*. 2023;11(8):722–732. doi:10.1002/ueg2.12442
7. Du L, Ha C. Epidemiology and pathogenesis of ulcerative colitis. *Gastroenterol Clin North Am*. 2020;49(4):643–654. doi:10.1016/j.gtc.2020.07.005
8. Li W, Zhao T, Wu D, et al. Colorectal cancer in ulcerative colitis: mechanisms, surveillance and chemoprevention. *Curr Oncol*. 2022;29(9):6091–6114. doi:10.3390/curroncol29090479
9. Glassner KL, Abraham BP, Quigley EMM. The microbiome and inflammatory bowel disease. *J Allergy Clin Immunol*. 2020;145(1):16–27. doi:10.1016/j.jaci.2019.11.003
10. Wangchuk P, Yeshi K, Loukas A. Ulcerative colitis: clinical biomarkers, therapeutic targets, and emerging treatments. *Trends Pharmacol Sci*. 2024;45(10):892–903. doi:10.1016/j.tips.2024.08.003
11. Dai Y, Lu Q, Li P, et al. Xianglian Pill attenuates ulcerative colitis through TLR4/MyD88/NF-κB signaling pathway. *J Ethnopharmacol*. 2023;300:115690. doi:10.1016/j.jep.2022.115690
12. Wang W, Jia S, Miao G, et al. Bioactive glass in the treatment of ulcerative colitis to regulate the TLR4 / MyD88 / NF-κB pathway. *Biomater Adv*. 2023;152:213520. doi:10.1016/j.bioadv.2023.213520
13. Mao X, Sun R, Wang Q, et al. l-isoleucine administration alleviates DSS-induced colitis by regulating TLR4/MyD88/NF-κB pathway in rats. *Front Immunol*. 2022;12:817583. doi:10.3389/fimmu.2021.817583
14. Li C, Ai G, Wang Y, et al. Oxyberberine, a novel gut microbiota-mediated metabolite of berberine, possesses superior anti-colitis effect: impact on intestinal epithelial barrier, gut microbiota profile and TLR4-MyD88-NF-κB pathway. *Pharmacol Res*. 2020;152:104603. doi:10.1016/j.phrs.2019.104603
15. Tao J, Huang Z, Wang Y, et al. Ethanolic extract from pteris wallichiana alleviates DSS-induced intestinal inflammation and intestinal barrier dysfunction by inhibiting the TLR4/NF-κB pathway and regulating tight junction proteins. *Molecules*. 2022;27(10):3093. doi:10.3390/molecules27103093
16. Shen ZH, Zhu CX, Quan YS, et al. Relationship between intestinal microbiota and ulcerative colitis: mechanisms and clinical application of probiotics and fecal microbiota transplantation. *World J Gastroenterol*. 2018;24(1):5–14. doi:10.3748/wjg.v24.i1.5
17. Guo P, Wang W, Xiang Q, et al. Engineered probiotic ameliorates ulcerative colitis by restoring gut microbiota and redox homeostasis. *Cell Host Microbe*. 2024;32(9):1502–1518.e9. doi:10.1016/j.chom.2024.07.028
18. Kataoka K. The intestinal microbiota and its role in human health and disease. *J Med Invest*. 2016;63(1–2):27–37. doi:10.2152/jmi.63.27

19. Foppa C, Rizkala T, Repici A, Hassan C, Spinelli A. Microbiota and IBD: current knowledge and future perspectives. *Dig Liver Dis*. 2024;56(6):911–922. doi:10.1016/j.dld.2023.11.015
20. Costello SP, Hughes PA, Waters O, et al. Effect of fecal microbiota transplantation on 8-week remission in patients with ulcerative colitis: a randomized clinical trial. *JAMA*. 2019;321(2):156–164. doi:10.1001/jama.2018.20046
21. Paramsothy S, Nielsen S, Kamm MA, et al. Specific bacteria and metabolites associated with response to fecal microbiota transplantation in patients with ulcerative colitis. *Gastroenterology*. 2019;156(5):1440–1454.e2. doi:10.1053/j.gastro.2018.12.001
22. Zong Y, Meng J, Mao T, Han Q, Zhang P, Shi L. Repairing the intestinal mucosal barrier of traditional Chinese medicine for ulcerative colitis: a review. *Front Pharmacol*. 2023;14:1273407. doi:10.3389/fphar.2023.1273407
23. Wang M, Fu R, Xu D, et al. Traditional Chinese Medicine: a promising strategy to regulate the imbalance of bacterial flora, impaired intestinal barrier and immune function attributed to ulcerative colitis through intestinal microecology. *J Ethnopharmacol*. 2024;318(Pt A):116879. doi:10.1016/j.jep.2023.116879
24. Qi Q, Liu YN, Lv SY, et al. Gut microbiome alterations in colitis rats after moxibustion at bilateral Tianshu acupoints. *BMC Gastroenterol*. 2022;22(1):62. doi:10.1186/s12876-022-02115-1
25. Wei G, Xie Y, Pei M, et al. A comparative metabolomics study between grain-sized moxibustion and suspended moxibustion on rats with gastric ulcers. *Heliyon*. 2023;9(8):e19108. doi:10.1016/j.heliyon.2023.e19108
26. Zhu Y, Zhuang Z, Wu Q, et al. CD39/CD73/A2a adenosine metabolic pathway: targets for moxibustion in treating DSS-induced ulcerative colitis. *Am J Chin Med*. 2021;49(3):661–676. doi:10.1142/S0192415X21500300
27. Guijun L, Yuedong L. 30 cases of ulcerative colitis with type of spleen & kidney Yang-deficiency treated by moxibustion with seed-sized moxa cone and mesalazine. *J External Treatment Trad Chinese Med*. 2018;27(06):16–17.
28. Tao Z, Jie L, Hao Y, et al. Effect of grain-sized moxibustion on JAK2/ STAT3 signaling pathway in colon tissue of ulcerative colitis mice. *J Traditional Chin Med*. 2024;65(18).
29. Wang H, Liu Z, Yu T, et al. The effect of tuina on ulcerative colitis model mice analyzed by gut microbiota and proteomics. *Front Microbiol*. 2022;13:976239. doi:10.3389/fmicb.2022.976239
30. Huang Q, Dong LC, Zhang RB, et al. Effect of electroacupuncture on Notch/NF-κB signaling pathway in colonic mucosa of mice with ulcerative colitis (in Chinese) [J]. *Acupuncture Res*. 2023;48(2):158–164. doi:10.13702/j.1000-0607.20211284
31. Li ZR. *Experimental Acupuncturology (in Chinese)*. 2nd ed. Beijing: China Press of Traditional Chinese Medicine; 2007.
32. Zhang Z, Li S, Cao H, et al. The protective role of phloretin against dextran sulfate sodium-induced ulcerative colitis in mice. *Food Funct*. 2019;10(1):422–431. doi:10.1039/C8FO01699B
33. Cooper HS, Murthy SN, Shah RS, Sedergran DJ. Clinicopathologic study of dextran sulfate sodium experimental murine colitis. *Lab Invest*. 1993;69(2):238–249.
34. Bessissow T, Lemmens B, Ferrante M, et al. Prognostic value of serologic and histologic markers on clinical relapse in ulcerative colitis patients with mucosal healing. *Am J Gastroenterol*. 2012;107(11):1684–1692. doi:10.1038/ajg.2012.301
35. Wang J, Jin Z, Zhang W, et al. The preventable efficacy of β-glucan against leptospirosis. *PLoS Negl Trop Dis*. 2019;13(11):e0007789. doi:10.1371/journal.pntd.0007789
36. MacCain WJ, Tuomanen EI. Mini-review: bioactivities of bacterial cell envelopes in the central nervous system. *Front Cell Infect Microbiol*. 2020;10:588378. doi:10.3389/fcimb.2020.588378
37. van der Giessen J, Binyamin D, Belogolovski A, et al. Modulation of cytokine patterns and microbiome during pregnancy in IBD. *Gut*. 2020;69(3):473–486. doi:10.1136/gutjnl-2019-318263
38. Zhu L, Lu X, Liu L, Voglmeir J, Zhong X, Yu Q. Akkermansia muciniphila protects intestinal mucosa from damage caused by S. pullorum by initiating proliferation of intestinal epithelium. *Vet Res*. 2020;51(1):34. doi:10.1186/s13567-020-00755-3
39. Ma TM, Xu N, Ma XD, Bai ZH, Tao X, Yan HC. Moxibustion regulates inflammatory mediators and colonic mucosal barrier in ulcerative colitis rats. *World J Gastroenterol*. 2016;22(8):2566–2575. doi:10.3748/wjg.v22.i8.2566
40. Zhu T, Zhang C, Ren J, et al. Antioxidative effect of wheat-grain moxibustion on cyclophosphamide-induced liver injury in mice based on Nrf2-Keap1 signaling pathway. *Zhongguo Zhen Jiu*. 2024;44(5):549–554. doi:10.13703/j.0255-2930.20231015-k0003
41. Czarnewski P, Parigi SM, Sorini C, et al. Conserved transcriptomic profile between mouse and human colitis allows unsupervised patient stratification. *Nat Commun*. 2019;10(1):2892. doi:10.1038/s41467-019-10769-x
42. Xu Y, Chen L, Hu X, et al. Brusatol ameliorates intestinal mucosal injury in ulcerative colitis via activating IL-22/STAT3 pathway. *Int Immunopharmacol*. 2025;153:114482. doi:10.1016/j.intimp.2025.114482
43. Liang J, Dai W, Liu C, et al. Gingerenone A attenuates ulcerative colitis via targeting IL-17RA to inhibit inflammation and restore intestinal barrier function. *Adv Sci*. 2024;11(28):e2400206. doi:10.1002/advs.202400206
44. Gan GL, Liu J, Chen WJ, et al. The diverse roles of the mucin gene cluster located on chromosome 11p15.5 in colorectal cancer. *Front Cell Dev Biol*. 2020;8:514. doi:10.3389/fcell.2020.00514
45. He S, Guo Y, Zhao J, Xu X, Wang N, Liu Q. Ferulic acid ameliorates lipopolysaccharide-induced barrier dysfunction via MicroRNA-200c-3p-mediated activation of PI3K/AKT pathway in Caco-2 cells. *Front Pharmacol*. 2020;11:376. doi:10.3389/fphar.2020.00376
46. Cui L, Guan X, Ding W, et al. Scutellaria baicalensis Georgi polysaccharide ameliorates DSS-induced ulcerative colitis by improving intestinal barrier function and modulating gut microbiota. *Int J Biol Macromol*. 2021;166:1035–1045. doi:10.1016/j.ijbiomac.2020.10.259
47. Zhang W, Shen ZY, Song HL, et al. Protective effect of bone marrow mesenchymal stem cells in intestinal barrier permeability after heterotopic intestinal transplantation. *World J Gastroenterol*. 2014;20(23):7442–7451. doi:10.3748/wjg.v20.i23.7442
48. Singh R, Chandrashekharappa S, Bodduluri SR, et al. Enhancement of the gut barrier integrity by a microbial metabolite through the Nrf2 pathway. *Nat Commun*. 2019;10(1):89. doi:10.1038/s41467-018-07859-7
49. Yao D, Dai W, Dong M, Dai C, Wu S. MUC2 and related bacterial factors: therapeutic targets for ulcerative colitis. *EBioMedicine*. 2021;74:103751. doi:10.1016/j.ebiom.2021.103751
50. Zhang W, Zou G, Li B, et al. Fecal microbiota transplantation (FMT) alleviates experimental colitis in mice by gut microbiota regulation. *J Microbiol Biotechnol*. 2020;30(8):1132–1141. doi:10.4014/jmb.2002.02044
51. Dmytriv TR, Storey KB, Lushchak VI. Intestinal barrier permeability: the influence of gut microbiota, nutrition, and exercise. *Front Physiol*. 2024;15:1380713. doi:10.3389/fphys.2024.1380713

52. Stojanov S, Berlec A, Štrukelj B. The influence of probiotics on the firmicutes/bacteroidetes ratio in the treatment of obesity and inflammatory bowel disease. *Microorganisms*. 2020;8(11):1715. doi:10.3390/microorganisms8111715
53. Nomura K, Ishikawa D, Okahara K, et al. Bacteroidetes species are correlated with disease activity in ulcerative colitis. *J Clin Med*. 2021;10 (8):1749. doi:10.3390/jcm10081749
54. Liu L, Xu M, Lan R, et al. Bacteroides vulgatus attenuates experimental mice colitis through modulating gut microbiota and immune responses. *Front Immunol*. 2022;13:1036196. doi:10.3389/fimmu.2022.1036196
55. Wu Y, Zhang X, Liu X, et al. Galactooligosaccharides and Limosilactobacillus reuteri synergistically alleviate gut inflammation and barrier dysfunction by enriching Bacteroides acidifaciens for pentadecanoic acid biosynthesis. *Nat Commun*. 2024;15(1):9291. doi:10.1038/s41467-024-53144-1
56. Shin NR, Whon TW, Bae JW. Proteobacteria: microbial signature of dysbiosis in gut microbiota. *Trends Biotechnol*. 2015;33(9):496–503. doi:10.1016/j.tibtech.2015.06.011
57. Mukhopadhya I, Hansen R, El-Omar EM, Hold GL. IBD-what role do Proteobacteria play? *Nat Rev Gastroenterol Hepatol*. 2012;9(4):219–230. doi:10.1038/nrgastro.2012.14
58. Qiu L, Yan C, Yang Y, et al. Morin alleviates DSS-induced ulcerative colitis in mice via inhibition of inflammation and modulation of intestinal microbiota. *Int Immunopharmacol*. 2024;140:112846. doi:10.1016/j.intimp.2024.112846
59. Qu S, Fan L, Qi Y, et al. Akkermansia muciniphila alleviates dextran sulfate sodium (DSS)-induced acute colitis by NLRP3 activation. *Microbiol Spectr*. 2021;9(2):e0073021. doi:10.1128/Spectrum.00730-21
60. Xie Q, Li H, Ma R, et al. Effect of Coptis chinensis franch and Magnolia officinalis on intestinal flora and intestinal barrier in a TNBS-induced ulcerative colitis rats model. *Phytomedicine*. 2022;97:153927. doi:10.1016/j.phymed.2022.153927
61. Niu C, Hu XL, Yuan ZW, et al. Pulsatilla decoction improves DSS-induced colitis via modulation of fecal-bacteria-related short-chain fatty acids and intestinal barrier integrity. *J Ethnopharmacol*. 2023;300:115741. doi:10.1016/j.jep.2022.115741